Advances in Continuous and Discrete Models

RESEARCH Open Access

Bifurcation and chaos in a discrete Holling–Tanner model with Beddington–DeAngelis functional response

Run Yang[1] and Jianglin Zhao[1*]

*Correspondence:
ws05101162@163.com
[1]Faculty of Science and Technology, Sichuan Minzu College, Kangding, China

Abstract

The dynamics of a discrete Holling–Tanner model with Beddington–DeAngelis functional response is studied. The permanence and local stability of fixed points for the model are derived. The center manifold theorem and bifurcation theory are used to show that the model can undergo flip and Hopf bifurcations. Codimension-two bifurcation associated with 1:2 resonance is analyzed by applying the bifurcation theory. Numerical simulations are performed not only to verify the correctness of theoretical analysis but to explore complex dynamical behaviors such as period-6, 7, 10, 12 orbits, a cascade of period-doubling, quasi-periodic orbits, and the chaotic sets. The maximum Lyapunov exponents validate the chaotic dynamical behaviors of the system. The feedback control method is considered to stabilize the chaotic orbits. These complex dynamical behaviors imply that the coexistence of predator and prey may produce very complex patterns.

Keywords: Discrete predator–prey system; Stability; Flip and Hopf bifurcation; 1:2 resonance; Chaos

1 Introduction

Predator–prey interactions can be universally observed in our ecological systems of the real world. The relationship between predator and prey occupies an important place in determining the evolution of ecological models. Due to their universal existence and real significance, predator–prey dynamics has long been studied and will continue to be one of the dominant fields in mathematical biology [1–4]. When the prey population is so large as the predator population, the Holling–Tanner model describes the dynamics of the predator species which feeds on its favorite food item as long as it is in abundant supply and grows logistically with an intrinsic growth rate and a carrying capacity proportional to the size of the prey [5]. The Holling–Tanner predator–prey model with Beddington–DeAngelis functional response was introduced in [6–9] as follows:

$$\begin{cases} \frac{du}{dt} = ru(1-\frac{u}{k}) - \frac{\alpha uv}{a+bu+cv}, \\ \frac{dv}{dt} = s[v(1-\frac{hv}{u})], \\ u(0) > 0, \qquad v(0) > 0, \end{cases} \tag{1}$$

where r, k, α, a, b, c, s, h are positive constants, and $u(t)$ and $v(t)$ represent the population size of prey and predator at time t, respectively. The prey grows logistically with carrying capacity k and intrinsic growth rate r in the absence of predator. The predator consumes the prey following the functional response of Beddington–DeAngelis type $\alpha uv/(a + bu + cv)$ and cv measures the mutual interference between predators [6–10]. α, a, b, and c indicate the consumption rate, the saturation constant, the saturation constant for an alternative prey, and the predator interference constant, respectively. The predator grows logistically with intrinsic growth rate s, and the carrying capacity u/h of the predator is proportional to the population size of the prey. h denotes the number of prey that is required to sustain one predator at equilibrium when v equals u/h. v/u measures the loss in the predator population because of the scarcity of its favorite food. hv/u is known as the Leslie–Gower term.

However, if the size of population was rarely small, or the population had no overlapping generation, or people studied population changes within certain intervals of time in an ecological system, the discrete-time model would exhibit better results than the continuous-time model [11–18]. Many results have shown that discrete-time models can produce far richer dynamical behaviors than those observed in continuous-time models [19–23]. In fact, Zhao and Yan [8] considered the discrete-time form of system (1) derived from the forward Euler difference scheme (see [13, 14, 16, 17, 23]). The discrete-time model displayed complex dynamics such as flip bifurcation, Hopf bifurcation, an invariant cycle, quasi-periodic orbits, and chaos. However, it is worth noting that the Euler discrete form of (1) is not realistic enough since there exist negative values of prey and predator population size for some parameter values or initial values, which imply that the discrete form has no biological meanings. Avoiding the negative solutions emerging from the discrete system by using the forward Euler scheme, the homogenous techniques (see [11, 22, 24–26]) are applied to obtain the discrete model corresponding to system (1). Assume that the average growth rates in both populations vary at the regular interval of time. By applying the method of piecewise constant arguments, we obtain the following modified system:

$$\begin{cases} \frac{1}{u(t)}\frac{du(t)}{dt} = r(1 - \frac{u([t])}{k}) - \frac{\alpha v([t])}{a+bu([t])+cv([t])}, \\ \frac{1}{v(t)}\frac{dv(t)}{dt} = s(1 - \frac{hv([t])}{u([t])}), \end{cases} \tag{2}$$

where $[t]$ denotes the integer part of t and $t \in [0, \infty)$. According to [18], we can integrate (2) on the interval $[n, n + 1)$, $n = 0, 1, 2, \ldots$, which yields

$$\begin{cases} u(t) = u_n \exp((r(1 - \frac{u_n}{k}) - \frac{\alpha v_n}{a+bu_n+cv_n})(t - n)), \\ v(t) = v_n \exp((s(1 - \frac{hv_n}{u_n}))(t - n)). \end{cases} \tag{3}$$

Taking $t \to n + 1$, we can obtain the following discrete-time model:

$$\begin{cases} u_{n+1} = u_n \exp(r(1 - \frac{u_n}{k}) - \frac{\alpha v_n}{a+bu_n+cv_n}), \\ v_{n+1} = v_n \exp(s(1 - \frac{hv_n}{u_n})). \end{cases} \tag{4}$$

The outline of this paper is as follows. Section 2 discusses the performance and local stability of fixed points for model (4). Section 3 gives sufficient conditions for the existence

of flip bifurcation and Hopf bifurcation. Section 4 discusses the 1:2 resonance bifurcation. Section 5 presents numerical simulations to check our results of theoretical analysis and exhibit some complex and new dynamical behaviors. Section 6 presents chaos control by using the state feedback control method. Section 7 gives a brief conclusion.

2 Permanence and stability of fixed points

Definition 2.1 System (4) is permanent if there exist two positive constants m and M such that

$$m \leq \lim_{n\to\infty} \inf(u_n, v_n) \leq \lim_{n\to\infty} \sup(u_n, v_n) \leq M$$

for each positive solution (u_n, v_n) of system (4).

In the following, we use Lemmas 2.1 and 2.2 from [27] to discuss the permanence of (4).

Proposition 2.1 *Every positive solution (u_n, v_n) of system (4) is uniformly bounded.*

Proof Assume that (u_n, v_n) is a positive solution of system (4). From the first part of system (4), we have

$$u_{n+1} \leq u_n \exp\left(r\left(1 - \frac{u_n}{k}\right)\right)$$

for $n = 0, 1, 2, \ldots$. If $u_0 > 0$, we thus have

$$\lim_{n\to\infty} \sup u_n \leq \frac{k}{r} \exp(r-1) := M_1.$$

As a result, for any $\epsilon > 0$, there exists an integer N such that $u_n \leq M_1 + \epsilon$ when $n > N$ and $n \in \mathbb{N}$. According to the second part of system (4), for $n > N$ and $n \in \mathbb{N}$, we obtain

$$v_{n+1} \leq v_n \exp\left(s\left(1 - \frac{hv_n}{M_1 + \epsilon}\right)\right).$$

If $v_0 > 0$, there is

$$\lim_{n\to\infty} \sup v_n \leq \frac{M_1 + \epsilon}{hs} \exp(s-1).$$

The arbitrariness of ϵ then implies that

$$\lim_{n\to\infty} \sup v_n \leq \frac{M_1}{hs} \exp(s-1) := M_2.$$

Then it follows that $\lim_{n\to\infty} \sup(u_n, v_n) \leq M$ for any $(u_0, v_0) \geq 0$, where $M = \max(M_1, M_2)$. This proof is complete. □

Proposition 2.2 *Let $\eta = r - \frac{\alpha}{c} > 0$. Then, for any positive solution (u_n, v_n) of system (4), there exists a positive constant satisfying*

$$\lim_{n\to\infty} \inf(u_n, v_n) \geq m,$$

where $m = \min\left(\frac{\eta(\eta-\rho M)}{\rho}, \frac{sm_1}{h} \exp\left(s - \frac{hsM}{m_1}\right)\right)$.

Proof Let (u_n, v_n) be a positive solution of system (4). From the first part of (4), it follows that

$$u_{n+1} \geq u_n \exp\left(r\left(1 - \frac{u_n}{k}\right) - \frac{\alpha}{c}\right) = u_n \exp(\eta - \rho u_n), \quad n = 0, 1, 2, \ldots,$$

where $\eta = r - \alpha/c$ and $\rho = r/k$. If $u_0 > 0$ and $\eta > 0$, we thus have

$$\liminf_{n\to\infty} u_n \geq \min\left\{\frac{\eta}{\rho}\exp(\eta - \rho M), \frac{\eta}{\rho}\right\} := m_1.$$

Consequently, for any $\epsilon > 0$, there exists an integer N such that $u_n \geq m_1 + \epsilon$ when $n > N$ and $n \in \mathbb{N}$. According to the second part of system (4), for $n > N$ and $n \in \mathbb{N}$, we therefore obtain

$$v_{n+1} \geq v_n \exp\left(s\left(1 - \frac{hv_n}{m_1 + \epsilon}\right)\right).$$

If $v_0 > 0$, there is

$$\liminf_{n\to\infty} v_n \geq \min\left\{\frac{s(m_1 + \epsilon)}{h}\exp\left(s - \frac{hsM}{m_1 + \epsilon}\right), \frac{s(m_1 + \epsilon)}{h}\right\}.$$

The arbitrariness of ϵ then implies that

$$\liminf_{n\to\infty} v_n \geq \min\left\{\frac{sm_1}{h}\exp\left(s - \frac{hsM}{m_1}\right), \frac{sm_1}{h}\right\} := m_2.$$

Then it follows that $\lim_{n\to\infty} \inf(u_n, v_n) \geq m$ for any $(u_0, v_0) > 0$, where $m = \min(m_1, m_2)$. This proof is complete. □

According to Propositions 2.1 and 2.2, system (4) is permanent if $r > \frac{\alpha}{c}$.

For all parameter values, system (4) has two fixed points, the boundary fixed point $A(k, 0)$, and the unique positive fixed point $B(u^*, v^*)$ defined by

$$u^* = \frac{\theta + \sqrt{\theta^2 + 4ahr^2k(bh + c)}}{2r(bh + c)}, \qquad v^* = \frac{u^*}{h},$$

where $\theta = crk + bhrk - k\alpha - ahr$.

In the next, we now perform the linear stability analysis of system (4) at each fixed point. The Jacobian matrix of system (4) evaluated at any equilibrium point (u, v) is given by

$$J(u, v) = \begin{pmatrix} \gamma_{11} & \gamma_{12} \\ \gamma_{21} & \gamma_{22} \end{pmatrix}.$$

Then the characteristic equation of $J(u, v)$ can be written as

$$\lambda^2 - (\gamma_{11} + \gamma_{22})\lambda + \gamma_{11}\gamma_{22} - \gamma_{21}\gamma_{12} = 0. \tag{5}$$

Proposition 2.3 *The eigenvalues of the boundary fixed point* $A(k,0)$ *are* $\lambda_1 = 1-r$ *and* $\lambda_2 = e^s$. *Then* $A(k,0)$ *is a saddle if* $0 < r < 2$. $A(k,0)$ *is a source if* $r > 2$. *And* $A(k,0)$ *is nonhyperbolic if* $r = 2$.

Let

$$F_A = \{(r,k,\alpha,a,b,c,s,h) \in \mathbb{R}^8 : r = 2\}.$$

Then it can be easily seen that one of the eigenvalues of $A(k,0)$ is -1 and the other $e^s > 1$ when all parameters locate in F_A. The center manifold of system (4) at $A(k,0)$ is $v = 0$ when parameters are in F_A. Therefore, system (4) restricted to this center manifold becomes: $u_{n+1} = u_n \exp(r(1-u/k))$. The system can enter into chaos through a period-doubling bifurcation as the bifurcation parameter r increases.

The characteristic equation of the Jacobian matrix $J(u,v)$ evaluated at the unique positive fixed point $B(u^*,v^*)$ can be written as

$$\lambda^2 - (2-s+G)\lambda + \left((1+G)(1-s) - \frac{H}{h}\right) = 0, \tag{6}$$

where

$$G = -\frac{ru^*}{k} + \frac{\alpha b u^* v^*}{(a+bu^*+cv^*)^2}, \qquad H = -\frac{\alpha s u^*(a+bu^*)}{(a+bu^*+cv^*)^2} < 0. \tag{7}$$

Suppose that λ_1 and λ_2 are two roots of (6).

Proposition 2.4 *The fixed point* $B(u^*,v^*)$ *is one of the following types in Table 1, where* G *and* H *are given by* (7).

3 Flip bifurcation and Hopf bifurcation

First we discuss the flip bifurcation of system (4) at the unique positive fixed point $B(u^*,v^*)$. Let us define

$$F_B = \left\{(r,k,\alpha,a,b,c,s,h) : h = h_1 = \frac{H}{(2+G)(2-s)}, s \neq G+4\right\}.$$

The two roots of (6) are $\lambda_1 = -1$ and $\lambda_2 = 3 + (G-s) \neq \pm 1$ when the parameters lie in F_B. Then the unique fixed point $B(u^*,v^*)$ of system (4) may undergo a flip bifurcation when parameters vary in a small neighborhood of F_B. Taking parameters $(r,k,\alpha,a,b,c,s,h) \in F_B$ and considering a small perturbation h^* ($|h^*| \ll 1$) of h_1 as a new dependent variable, system (4) can be described by the following map:

$$\begin{pmatrix} u \\ h^* \\ v \end{pmatrix} \longmapsto \begin{pmatrix} u\exp(r(1-\frac{u}{k}) - \frac{\alpha v}{a+bu+cv}) \\ h^* \\ v\exp(s(1-\frac{(h_1+h^*)v}{u})) \end{pmatrix}. \tag{8}$$

Assume that $U = u - u^*$ and $V = v - v^*$. Then the fixed point $B(u^*,v^*)$ of map (8) is transformed into the origin. We rewrite respectively U and V as u and v, then map (8)

Table 1 Properties of the fixed point $B(u^*, v^*)$

Conditions	Eigenvalues	Properties
$G < s < G + 4$ $\max\{-\frac{Gs}{H}, \frac{(2+G)(2-s)}{H}\} < \frac{1}{h} \leq -\frac{(G+s)^2}{4H}$	$-1 < \lambda_{1,2} < 1$	stable node
$G > s$ $-\frac{Gs}{H} < \frac{1}{h} \leq -\frac{(G+s)^2}{4H}$	$\lambda_{1,2} > 1$	unstable node
$G + 4 < s$ $\frac{(2+G)(2-s)}{H} < \frac{1}{h} \leq -\frac{(G+s)^2}{4H}$	$\lambda_{1,2} < -1$	unstable node
$G < s$ $-\frac{Gs}{H} < \frac{1}{h} < \frac{(2+G)(2-s)}{H}$ $\frac{1}{h} \leq -\frac{(G+s)^2}{4H}$	$\lambda_1 < -1, -1 < \lambda_2 < 1$	unstable saddle
$\frac{1}{h} > -\frac{(G+s)^2}{4H}$ $\frac{(1+G)(1-s)}{H} < \frac{1}{h} < \frac{G-s-Gs}{H}$	conjugate complex roots $\lvert\lambda_{1,2}\rvert < 1$	stable focus
$\frac{1}{h} > \max\{-\frac{(G+s)^2}{4H}, \frac{G-s-Gs}{H}\}$	conjugate complex roots $\lvert\lambda_{1,2}\rvert > 1$	unstable focus
$\frac{1}{h} = \frac{(2+G)(2-s)}{H}$ $s \neq G + 4$	$\lambda_1 = -1, \lambda_2 \neq -1$	nonhyperbolic
$\frac{1}{h} = \frac{(2+G)(2-s)}{H}$ $s = G + 4$	$\lambda_{1,2} = -1$	nonhyperbolic
$\frac{1}{h} = \frac{G-s-Gs}{H}$ $G < s < G + 4$	conjugate complex roots $\lvert\lambda_{1,2}\rvert = 1$	nonhyperbolic

becomes

$$\begin{pmatrix} u \\ h^* \\ v \end{pmatrix} \longmapsto \begin{pmatrix} a_{11} & 0 & a_{13} \\ 0 & 1 & 0 \\ a_{31} & a_{32} & a_{33} \end{pmatrix} \begin{pmatrix} u \\ h^* \\ v \end{pmatrix} + \begin{pmatrix} f_1(u, v, h^*) \\ 0 \\ f_2(u, v, h^*) \end{pmatrix}, \tag{9}$$

where

$$\begin{aligned}
&f_1\big(u, v, h^*\big) = a_{14}u^2 + a_{15}uv + a_{16}v^2 + O\big(\big(|u| + |v|\big)^3\big),\\
&f_2\big(u, v, h^*\big) = a_{34}u^2 + a_{35}uv + a_{36}v^2 + e_1uh^* + e_2vh^* + e_3h_*^2 + O\big(\big(|u| + |v| + \big|h^*\big|\big)^3\big),\\
&a_{11} = 1 + G, \qquad a_{13} = \frac{H}{s}, \qquad a_{31} = \frac{s}{h_1}, \qquad a_{32} = -\frac{su^*}{h_1^2}, \qquad a_{33} = 1 - s,\\
&a_{14} = \frac{G^2 + 2G}{2u^*} - \frac{\alpha b^2 u^* v^*}{(a + bu^* + cv^*)^3}, \qquad a_{15} = \frac{H(1 + G)}{su^*} + \frac{\alpha bu(a + bu^* - cv^*)}{(a + bu^* + cv^*)^3},\\
&a_{16} = \frac{H^2}{2s^2u^*} - \frac{cH}{s(a + bu^* + cv^*)}, \qquad a_{34} = \frac{s^2 - 2s}{2h_1u^*}, \qquad a_{35} = \frac{2s - s^2}{u^*},\\
&a_{36} = \frac{h_1s(s - 2)}{2u^*}, \qquad e_1 = \frac{s - s^2}{h_1^2}, \qquad e_2 = \frac{s^2 - 2s}{h_1}, \qquad e_3 = \frac{s^2}{2h_1^3}.
\end{aligned} \tag{10}$$

Let us define the following matrix:

$$T = \begin{pmatrix} a_{13} & a_{13}a_{32} & a_{13} \\ 0 & 2(1 - \lambda_2) & 0 \\ -a_{11} - 1 & (1 - a_{11})a_{32} & \lambda_2 - a_{11} \end{pmatrix}.$$

Then $\det(A) = 2a_{13}(1-\lambda_2^2) \neq 0$. So, T is an invertible matrix. Moreover, $T^{-1} = \frac{1}{\det(T)}\operatorname{adj}(T)$. Applying the transformation $(u, h^*, v)^T = T(\tilde{u}, \tilde{h^*}, \tilde{v})^T$, map (9) can be rewritten as

$$\begin{pmatrix} \tilde{u} \\ \tilde{h^*} \\ \tilde{v} \end{pmatrix} \longmapsto \begin{pmatrix} -1 & 0 & 0 \\ 0 & 1 & 0 \\ 0 & 0 & \lambda_2 \end{pmatrix} \begin{pmatrix} \tilde{u} \\ \tilde{h^*} \\ \tilde{v} \end{pmatrix} + \begin{pmatrix} g_1(\tilde{u}, \tilde{v}, \tilde{h^*}) \\ 0 \\ g_2(\tilde{u}, \tilde{v}, \tilde{h^*}) \end{pmatrix}, \tag{11}$$

where

$$\begin{aligned} g_1\big(\tilde{u}, \tilde{v}, \tilde{h^*}\big) &= \frac{a_{14}(a_{11}-\lambda_2) - a_{13}a_{34}}{a_{13}(1+\lambda_2)}u^2 + \frac{a_{15}(a_{11}-\lambda_2) - a_{13}a_{35}}{a_{13}(1+\lambda_2)}uv \\ &\quad + \frac{a_{16}(a_{11}-\lambda_2) - a_{13}a_{36}}{a_{13}(1+\lambda_2)}v^2 - \frac{e_1}{(1+\lambda_2)}uh^* - \frac{e_2}{(1+\lambda_2)}vh^* - \frac{e_3}{1+\lambda_2}h^{*2} \\ &\quad + O\big(\big(|\tilde{u}| + |\tilde{v}| + |\tilde{h^*}|\big)^3\big), \\ g_2\big(\tilde{u}, \tilde{v}, \tilde{h^*}\big) &= \frac{a_{14}(1+a_{11}) + a_{13}a_{34}}{a_{13}(1+\lambda_2)}u^2 + \frac{a_{15}(1+a_{11}) + a_{13}a_{35}}{a_{13}(1+\lambda_2)}uv \\ &\quad + \frac{a_{16}(1+a_{11}) + a_{13}a_{36}}{a_{13}(1+\lambda_2)}v^2 + \frac{e_1}{1+\lambda_2}uh^* + \frac{e_2}{1+\lambda_2}vh^* + \frac{e_3}{1+\lambda_2}h^{*2} \\ &\quad + O\big(\big(|\tilde{u}| + |\tilde{v}| + |\tilde{h^*}|\big)^3\big), \end{aligned}$$

with $u = a_{13}\tilde{u} + a_{13}a_{32}\tilde{h^*} + a_{13}\tilde{v}$, $h^* = 2(1-\lambda_2)\tilde{h^*}$ and $v = -(1+a_{11})\tilde{u} + (1-a_{11})a_{32}\tilde{h^*} + (\lambda_2 - a_{11})\tilde{v}$.

The center manifold theorem is applied to determine the dynamics of $(\tilde{u}, \tilde{v}) = (0,0)$ at $\tilde{h^*} = 0$. Then there exists a center manifold of map (11), which can be represented as

$$W^c(0,0) = \big\{(\tilde{u}, \tilde{v}) | \tilde{v} = \beta\big(\tilde{u}, \tilde{h^*}\big), \beta(0,0) = 0, D\beta(0,0) = 0\big\}.$$

Assume that

$$\beta\big(\tilde{u}, \tilde{h^*}\big) = a_1\tilde{u}^2 + a_2\tilde{u}\tilde{h^*} + a_3\tilde{h^*}^2 + O\big(\big(|\tilde{u}| + |\tilde{h^*}|\big)^3\big). \tag{12}$$

Then the center manifold implies that

$$\beta\big(-\tilde{u} + g_1\big(\tilde{u}, \beta\big(\tilde{u}, \tilde{h^*}\big), \tilde{h^*}\big), \tilde{h^*}\big) - \lambda_2\beta\big(\tilde{u}, \tilde{h^*}\big) - g_2\big(\tilde{u}, \beta\big(\tilde{u}, \tilde{h^*}\big), \tilde{h^*}\big) = 0. \tag{13}$$

Substituting (11) and (12) into (13) and comparing the coefficients of (13), it follows that

$$\begin{aligned} a_1 &= \frac{1}{a_{13}(1-\lambda_2^2)}\big\{a_{13}^2\big[a_{14}(1+a_{11}) + a_{13}a_{34}\big] - a_{13}(1+a_{11})\big[a_{15}(1+a_{11}) + a_{13}a_{35}\big] \\ &\quad + (1+a_{11})^2\big[a_{16}(1+a_{11}) + a_{13}a_{36}\big]\big\}, \\ a_2 &= -\frac{2}{a_{13}(1+\lambda_2)^2}\big\{a_{13}^2a_{32}\big[a_{14}(1+a_{11}) + a_{13}a_{34}\big] - a_{11}a_{13}a_{32}\big[a_{15}(1+a_{11}) + a_{13}a_{35}\big] \\ &\quad - a_{32}\big(1-a_{11}^2\big)\big[a_{16}(1+a_{11}) + a_{13}a_{36}\big] + e_1a_{13}^2(1-\lambda_2) - e_2a_{13}(1+a_{11})(1-\lambda_2)\big\}, \end{aligned}$$

$$
\begin{aligned}
a_3 = {} & \frac{1}{a_{13}(1-\lambda_2^2)}\big\{a_{13}^2a_{32}^2\big[a_{14}(1+a_{11})+a_{13}a_{34}\big] \\
& + a_{13}a_{32}^2(1-a_{11})\big[a_{15}(1+a_{11})+a_{13}a_{35}\big] \\
& + a_{32}^2(1-a_{11})^2\big[a_{16}(1+a_{11})+a_{13}a_{36}\big] + 2e_1a_{13}^2a_{32}(1-\lambda_2) \\
& + 2e_2a_{13}a_{32}(1-a_{11})(1-\lambda_2) + 4e_3a_{13}(1-\lambda_2)^2\big\}.
\end{aligned}
$$

Therefore, system (11) restricted to the center manifold $W^c(0,0)$ is given by

$$
F:\tilde{u}\mapsto -\tilde{u}+k_1\tilde{u}^2+k_2\tilde{u}\tilde{h^*}+k_3\tilde{h^*}^2+k_4\tilde{u}^2\tilde{h^*}+k_5\tilde{u}\tilde{h^*}^2+k_6\tilde{u}^3+k_7\tilde{h^*}^3+O\big(\big(|\tilde{u}|+|\tilde{h^*}|\big)^4\big),
$$

where

$$
\begin{aligned}
k_1 = {} & \frac{1}{a_{13}(1+\lambda_2)}\big\{a_{13}^2\big[a_{14}(a_{11}-\lambda_2)+a_{13}a_{34}\big]-a_{13}(1+a_{11})\big[a_{15}(a_{11}-\lambda_2)+a_{13}a_{35}\big] \\
& + (1+a_{11})^2\big[a_{16}(a_{11}-\lambda_2)+a_{13}a_{36}\big]\big\}, \\
k_2 = {} & \frac{2}{a_{13}(1+\lambda_2)}\big\{a_{13}^2a_{32}\big[a_{14}(a_{11}-\lambda_2)+a_{13}a_{34}\big]-a_{11}a_{13}a_{32}\big[a_{15}(a_{11}-\lambda_2)+a_{13}a_{35}\big] \\
& - a_{32}\big(1-a_{11}^2\big)\big[a_{16}(a_{11}-\lambda_2)+a_{13}a_{36}\big]-e_1a_{13}^2(1-\lambda_2)+e_2a_{13}(1+a_{11})(1-\lambda_2)\big\}, \\
k_3 = {} & \frac{1}{a_{13}(1+\lambda_2)}\big\{a_{13}^2a_{32}^2\big[a_{14}(a_{11}-\lambda_2)+a_{13}a_{34}\big] \\
& + a_{13}a_{32}^2(1-a_{11})\big[a_{15}(a_{11}-\lambda_2)+a_{13}a_{35}\big] \\
& + a_{32}^2(1-a_{11})^2\big[a_{16}(a_{11}-\lambda_2)+a_{13}a_{36}\big]-2e_1a_{13}^2a_{32}(1-\lambda_2) \\
& - 2e_2a_{13}a_{32}(1-a_{11})(1-\lambda_2)-4e_3a_{13}(1-\lambda_2)^2\big\}, \\
k_4 = {} & \frac{1}{a_{13}(1+\lambda_2)}\big\{\big[2a_1a_{13}^2a_{32}+2a_2a_{13}^2\big]\big[a_{14}(a_{11}-\lambda_2)+a_{13}a_{34}\big] \\
& + \big[a_1a_{13}a_{32}(\lambda_2+1-2a_{11})+a_2a_{13}(\lambda_2-1-2a_{11})\big]\big[a_{15}(a_{11}-\lambda_2)+a_{13}a_{35}\big] \\
& + \big[2a_1a_{32}(1-a_{11})(\lambda_2-a_{11})-2a_2(1+a_{11})(\lambda_2-a_{11})\big]\big[a_{16}(a_{11}-\lambda_2)+a_{13}a_{36}\big] \\
& - 2a_1e_1a_{13}^2(1-\lambda_2)-2a_1e_2a_{13}(\lambda_2-a_{11})(1-\lambda_2)\big\}, \\
k_5 = {} & \frac{1}{a_{13}(1+\lambda_2)}\big\{2a_{13}^2a_2a_{32}\big[a_{14}(a_{11}-\lambda_2)+a_{13}a_{34}\big] \\
& + \big[a_3a_{13}(\lambda_2-2a_{11}+1)+a_2a_{13}a_{32}(\lambda_2+1-2a_{11})\big]\big[a_{15}(a_{11}-\lambda_2)+a_{13}a_{35}\big] \\
& + \big[2a_2a_{32}(1-a_{11})(\lambda_2-a_{11})-2a_3(1+a_{11})(\lambda_2-a_{11})\big]\big[a_{16}(a_{11}-\lambda_2)+a_{13}a_{36}\big] \\
& - 2a_2e_1a_{13}^2(1-\lambda_2)-2a_2e_2a_{13}(\lambda_2-a_{11})(1-\lambda_2)\big\}, \\
k_6 = {} & \frac{a_1}{a_{13}(1+\lambda_2)}\big\{2a_{13}^2\big[a_{14}(a_{11}-\lambda_2) \\
& + a_{13}a_{34}\big]+a_{13}(\lambda_2-2a_{11}-1)\big[a_{15}(a_{11}-\lambda_2)+a_{13}a_{35}\big] \\
& - 2(1+a_{11})(\lambda_2-a_{11})\big[a_{16}(a_{11}-\lambda_2)+a_{13}a_{36}\big]\big\}, \\
k_7 = {} & \frac{a_3}{a_{13}(1+\lambda_2)}\big\{2a_{13}^2a_{32}\big[a_{14}(a_{11}-\lambda_2)+a_{13}a_{34}\big] \\
& + a_{13}a_{32}(\lambda_2-2a_{11}+1)\big[a_{15}(a_{11}-\lambda_2)+a_{13}a_{35}\big]
\end{aligned}
$$

$$+ 2a_{32}(1-a_{11})(\lambda_2 - a_{11})\big[a_{16}(a_{11}-\lambda_2) + a_{13}a_{36}\big]$$
$$- 2e_1 a_{13}^2(1-\lambda_2) - 2e_2 a_{13}(1-\lambda_2)(\lambda_2 - a_{11})\big\}.$$

Assume that

$$\mu_1 = \left(\frac{\partial^2 F}{\partial\tilde{u}\partial\tilde{h}^*} + \frac{1}{2}\frac{\partial F}{\partial\tilde{h}^*}\frac{\partial^2 F}{\partial^2\tilde{u}}\right)\Big|_{(0,0)} = k_2, \qquad \mu_2 = \left(\frac{1}{6}\frac{\partial^3 F}{\partial^3\tilde{u}} + \left(\frac{1}{2}\frac{\partial^2 F}{\partial^2\tilde{u}}\right)^2\right)\Big|_{(0,0)} = k_6 + k_1^2.$$

Theorem 3.1 *If $\mu_1 \neq 0$ and $\mu_2 \neq 0$, then system (4) can undergo a flip bifurcation at $B(u^*, v^*)$ when the parameter h varies in a small neighborhood of F_B. Moreover, if $\mu_2 > 0$ (resp., $\mu_2 < 0$), then the period-2 orbits that bifurcate from $B(u^*, v^*)$ are stable (resp., unstable).*

In the following, we focus on the Hopf bifurcation of system (4) at $B(u^*, v^*)$. Assume that

$$H_B = \left\{(r, k, \alpha, a, b, c, s, h) : h = h_2 = \frac{H}{G - s - Gs}, G < s < G + 4\right\}.$$

Then (6) has two complex conjugate roots on the unit circle, which implies that system (4) at $B(u^*, v^*)$ may undergo a Hopf bifurcation when all parameters vary in a small neighborhood of H_B. Taking parameters $(r, k, \alpha, a, b, c, s, h) \in H_B$ and considering a small perturbation h_* ($|h_*| \ll 1$) of h_2 as a new dependent variable, system (4) can be described by the following map:

$$\begin{pmatrix} u \\ v \end{pmatrix} \longmapsto \begin{pmatrix} u\exp(r(1-\frac{u}{k}) - \frac{\alpha v}{(a+bu+cv)^2}) \\ v\exp(s(1-\frac{(h_2+h_*)v}{u})) \end{pmatrix}. \tag{14}$$

Assume that $U = u - u^*$ and $V = v - v^*$. Then the fixed point $B(u^*, v^*)$ of map (14) is transformed into the origin. For convenience, U and V are still rewritten as u and v, respectively. Then we have

$$\begin{pmatrix} u \\ v \end{pmatrix} \longmapsto \begin{pmatrix} c_{11} & c_{12} \\ c_{21} & c_{22} \end{pmatrix}\begin{pmatrix} u \\ v \end{pmatrix} + \begin{pmatrix} M_1(u, v) \\ M_2(u, v) \end{pmatrix}, \tag{15}$$

where

$$M_1(u, v) = c_{13}u^2 + c_{14}uv + c_{15}v^2 + c_{16}u^3 + c_{17}u^2v + c_{18}uv^2 + c_{19}v^3 + O\big(\big(|u| + |v|\big)^4\big),$$
$$M_2(u, v) = c_{23}u^2 + c_{24}uv + c_{25}v^2 + c_{26}u^3 + c_{27}u^2v + c_{28}uv^2 +_{29} v^3 + +O\big(\big(|u| + |v|\big)^4\big),$$
$$c_{11} = 1 + G, \qquad c_{12} = \frac{H}{s}, \qquad c_{21} = \frac{s}{h}, \qquad c_{22} = 1 - s,$$
$$c_{13} = \frac{G^2 + 2G}{2u^*} - \frac{\alpha b^2 u^* v^*}{(a + bu^* + cv*)^2}, \qquad c_{14} = \frac{G(H+1)}{su^*} + \frac{\alpha b(a + bu^* - cv^*)}{(a + bu^* + cv^*)^3},$$
$$c_{23} = \frac{s^2 - 2s}{2hu^*}, \qquad c_{24} = \frac{2s - s^2}{u^*}, \qquad c_{25} = \frac{hs^2 - 2hs}{2u^*},$$
$$c_{15} = \frac{H^2}{2s^2u^*} - \frac{cH}{s(a + bu^* + cv^*)},$$

$$
\begin{aligned}
c_{16} &= \frac{G^3+3G^2}{6u_*^2} - \frac{\alpha b^2 G v^*}{(a+bu^*+cv^*)^3} - \frac{\alpha b^2(a+cv^*)v^*}{(a+bu^*+cv^*)^4},\\
c_{17} &= \frac{G^2H+2GH}{2su_*^2} - \frac{\alpha b^2(u^*+Hv^*/s)}{(a+bu^*+cv^*)^3} + \frac{\alpha b(G+1)(a+bu^*-cv^*)}{(a+bu^*+cv^*)^3} + \frac{3\alpha b^2 u^* v^* c}{(a+bu^*+cv^*)^4},\\
c_{18} &= \frac{GH^2+H^2}{2s^2u_*^2} - \frac{cGH+cH}{s(a+bu^*+cv^*)u^*} + \frac{\alpha bH(a+bu^*-cv^*)}{s(a+bu^*+cv^*)^3}\\
&\quad - \frac{\alpha bcu^*(2a+2bu^*-cv^*)}{(a+bu^*+cv^*)^4},\\
c_{19} &= \frac{H^3}{6s^3u_*^2} - \frac{cH^2}{su^*(a+bu^*+cv^*)} + \frac{c^2H}{s(a+bu^*+cv^*)^2}, \qquad c_{26} = \frac{6s-6s^2+s^3}{6hu_*^2}v,\\
c_{27} &= \frac{5s^2-2s-s^3}{2u_*^2}, \qquad c_{28} = \frac{2hs-4hs^2+hs^3}{2u_*^2}, \qquad c_{29} = \frac{3h^2s^2-h^2s^3}{6u_*^2},
\end{aligned}
$$

with $h = h_2 + h_*$.

Then the characteristic equation associated with the linearization of map (15) at $(0,0)$ is given by

$$\lambda^2 - p(h_*)\lambda + q(h_*) = 0, \tag{16}$$

where

$$p(h_*) = c_{11} + c_{22}, q(h_*) = c_{11}c_{22} - c_{12}c_{21}.$$

When $h_* = 0$, there exists a pair of complex conjugate eigenvalues $\lambda, \bar{\lambda}$ of (16) with $|\lambda| = 1$. Then it has

$$\lambda, \bar{\lambda} = \frac{p(0) \pm \mathrm{i}\sqrt{4q(0)-p^2(0)}}{2}.$$

Furthermore, it implies that

$$|\lambda| = \sqrt{q(0)}, \qquad \left.\frac{d|\lambda|}{dh_*}\right|_{h_*=0} = \frac{H}{h_2^2} < 0.$$

It also requires $\lambda^n, \bar{\lambda}^n \neq 1$, $n = 1,2,3,4$ when $h_* = 0$. Equivalently, $p(0) \neq -2, 0, 1, 2$. Notice that $(r,k,\alpha,a,b,c,s,h) \in H_B$ implies $-2 < p(0) < 2$. It therefore needs to be $p(0) \neq 0, 1$, which leads to

$$G - s \neq -1, -2. \tag{17}$$

Accordingly, a pair of complex conjugate eigenvalues $\lambda, \bar{\lambda}$ of (16) does not lay in intersection of the unit circle with the coordinate axes.

Assume that $\rho = \mathrm{Re}(\lambda)$, $\omega = \mathrm{Im}(\lambda)$. Consider the following transformation:

$$\begin{pmatrix} u \\ v \end{pmatrix} = \begin{pmatrix} c_{12} & 0 \\ \rho - c_{11} & -\omega \end{pmatrix} \begin{pmatrix} \tilde{u} \\ \tilde{v} \end{pmatrix}.$$

Then the normal form of (15) can be presented as

$$\begin{pmatrix}\tilde{u}\\ \tilde{v}\end{pmatrix}\longmapsto\begin{pmatrix}\rho & -\omega\\ \omega & \rho\end{pmatrix}\begin{pmatrix}\tilde{u}\\ \tilde{v}\end{pmatrix}+\begin{pmatrix}\tilde{F}(\tilde{u},\tilde{v})\\ \tilde{G}(\tilde{u},\tilde{v})\end{pmatrix}, \tag{18}$$

where

$$\begin{aligned}\tilde{F}(\tilde{u},\tilde{v}) &= \frac{1}{c_{12}}\left(c_{13}u^2+c_{14}uv+c_{15}v^2+c_{16}u^3+c_{17}u^2v+c_{18}uv^2+c_{19}v^3\right)+O\left(\left(|\tilde{u}|+|\tilde{v}|\right)^4\right),\\ \tilde{G}(\tilde{u},\tilde{v}) &= \frac{((\rho-c_{11})c_{13}-c_{12}c_{23})}{\omega c_{12}}u^2+\frac{((\rho-c_{11})c_{14}-c_{12}c_{24})}{\omega c_{12}}uv\\ &\quad+\frac{((\rho-c_{11})c_{15}-c_{12}c_{25})}{\omega c_{12}}v^2+\frac{((\rho-c_{11})c_{16}-c_{12}c_{26})}{\omega c_{12}}u^3\\ &\quad+\frac{((\rho-c_{11})c_{17}-c_{12}c_{27})}{\omega c_{12}}u^2v+\frac{((\rho-c_{11})c_{18}-c_{12}c_{28})}{\omega c_{12}}uv^2\\ &\quad+\frac{((\rho-c_{11})c_{19}-c_{12}c_{29})}{\omega c_{12}}v^3+O\left(\left(|\tilde{u}|+|\tilde{v}|\right)^4\right),\end{aligned}$$

and $u=c_{12}\tilde{u}$, $v=(\rho-c_{11})\tilde{u}-\omega\tilde{v}$.

Let us denote

$$\begin{aligned}&\tilde{F}_{\tilde{u}\tilde{u}}=\left.\frac{\partial^2\tilde{F}(\tilde{u},\tilde{v})}{\partial^2\tilde{u}}\right|_{(\tilde{u},\tilde{v})=(0,0)},\qquad \tilde{F}_{\tilde{u}\tilde{v}}=\left.\frac{\partial^2\tilde{F}(\tilde{u},\tilde{v})}{\partial\tilde{u}\partial\tilde{v}}\right|_{(\tilde{u},\tilde{v})=(0,0)},\\ &\tilde{F}_{\tilde{v}\tilde{v}}=\left.\frac{\partial^2\tilde{F}(\tilde{u},\tilde{v})}{\partial^2\tilde{v}}\right|_{(\tilde{u},\tilde{v})=(0,0)},\qquad \tilde{F}_{\tilde{u}\tilde{u}\tilde{u}}=\left.\frac{\partial^3\tilde{F}(\tilde{u},\tilde{v})}{\partial^3\tilde{u}}\right|_{(\tilde{u},\tilde{v})=(0,0)},\\ &\tilde{F}_{\tilde{u}\tilde{u}\tilde{v}}=\left.\frac{\partial^3\tilde{F}(\tilde{u},\tilde{v})}{\partial^2\tilde{u}\partial\tilde{v}}\right|_{(\tilde{u},\tilde{v})=(0,0)},\qquad \tilde{F}_{\tilde{v}\tilde{v}\tilde{u}}=\left.\frac{\partial^3\tilde{F}(\tilde{u},\tilde{v})}{\partial^2\tilde{v}\partial\tilde{u}}\right|_{(\tilde{u},\tilde{v})=(0,0)},\\ &\tilde{F}_{\tilde{v}\tilde{v}\tilde{v}}=\left.\frac{\partial^3\tilde{F}(\tilde{u},\tilde{v})}{\partial^3\tilde{v}}\right|_{(\tilde{u},\tilde{v})=(0,0)},\qquad \tilde{G}_{\tilde{u}\tilde{u}}=\left.\frac{\partial^2\tilde{G}(\tilde{u},\tilde{v})}{\partial^2\tilde{u}}\right|_{(\tilde{u},\tilde{v})=(0,0)},\\ &\tilde{G}_{\tilde{u}\tilde{v}}=\left.\frac{\partial^2\tilde{G}(\tilde{u},\tilde{v})}{\partial\tilde{u}\partial\tilde{u}}\right|_{(\tilde{u},\tilde{v})=(0,0)},\qquad \tilde{G}_{\tilde{v}\tilde{v}}=\left.\frac{\partial^2\tilde{F}(\tilde{u},\tilde{v})}{\partial^2\tilde{v}}\right|_{(\tilde{u},\tilde{v})=(0,0)},\\ &\tilde{G}_{\tilde{u}\tilde{u}\tilde{u}}=\left.\frac{\partial^3\tilde{G}(\tilde{u},\tilde{v})}{\partial^3\tilde{u}}\right|_{(\tilde{u},\tilde{v})=(0,0)},\qquad \tilde{G}_{\tilde{u}\tilde{u}\tilde{v}}=\left.\frac{\partial^3\tilde{G}(\tilde{u},\tilde{v})}{\partial^2\tilde{u}\partial\tilde{v}}\right|_{(\tilde{u},\tilde{v})=(0,0)},\\ &\tilde{G}_{\tilde{v}\tilde{v}\tilde{u}}=\left.\frac{\partial^3\tilde{G}(\tilde{u},\tilde{v})}{\partial^2\tilde{v}\partial\tilde{u}}\right|_{(\tilde{u},\tilde{v})=(0,0)},\qquad \tilde{G}_{\tilde{v}\tilde{v}\tilde{v}}=\left.\frac{\partial^3\tilde{G}(\tilde{u},\tilde{v})}{\partial^3\tilde{v}}\right|_{(\tilde{u},\tilde{v})=(0,0)}.\end{aligned}$$

Then map (20) can undergo a Hopf bifurcation if the following discriminatory quantity is not zero:

$$l=\left[-\operatorname{Re}\left(\frac{(1-2\lambda)\bar{\lambda}^2}{1-\lambda}\xi_{11}\xi_{20}\right)-\frac{1}{2}|\xi_{11}|^2-|\xi_{02}|^2+\operatorname{Re}(\bar{\lambda}\xi_{21})\right]\Big|_{h_*=0}, \tag{19}$$

where

$$\xi_{20}=\frac{1}{8}\left[(\tilde{F}_{\tilde{u}\tilde{u}}-\tilde{F}_{\tilde{v}\tilde{v}}+2\tilde{G}_{\tilde{u}\tilde{v}})+\mathrm{i}(\tilde{G}_{\tilde{u}\tilde{u}}-\tilde{G}_{\tilde{v}\tilde{v}}-2\tilde{F}_{\tilde{u}\tilde{v}})\right],$$

$$\xi_{11} = \frac{1}{4}\big[(\tilde{F}_{\tilde{u}\tilde{u}} + \tilde{F}_{\tilde{v}\tilde{v}}) + \mathrm{i}(\tilde{G}_{\tilde{u}\tilde{u}} + \tilde{G}_{\tilde{v}\tilde{v}})\big],$$

$$\xi_{02} = \frac{1}{8}\big[(\tilde{F}_{\tilde{u}\tilde{u}} - \tilde{F}_{\tilde{v}\tilde{v}} - 2\tilde{G}_{\tilde{u}\tilde{v}}) + \mathrm{i}(\tilde{G}_{\tilde{u}\tilde{u}} - \tilde{G}_{\tilde{v}\tilde{v}} + 2\tilde{F}_{\tilde{u}\tilde{v}})\big],$$

$$\xi_{21} = \frac{1}{16}\big[(\tilde{F}_{\tilde{u}\tilde{u}\tilde{u}} + \tilde{F}_{\tilde{u}\tilde{v}\tilde{v}} + \tilde{G}_{\tilde{u}\tilde{u}\tilde{v}} + \tilde{G}_{\tilde{v}\tilde{v}\tilde{v}}) + \mathrm{i}(\tilde{G}_{\tilde{u}\tilde{u}\tilde{u}} + \tilde{G}_{\tilde{u}\tilde{v}\tilde{v}} - \tilde{F}_{\tilde{u}\tilde{u}\tilde{v}} - \tilde{F}_{\tilde{v}\tilde{v}\tilde{v}})\big].$$

Theorem 3.2 *If condition* (17) *holds and* $l \neq 0$, *then map* (4) *undergoes a Hopf bifurcation at* $B(u^*, v^*)$ *when the parameter* h *varies in a small neighborhood of* H_B. *Moreover, if* $l < 0$ (*resp.*, $l > 0$), *then an attracting* (*resp.*, *repelling*) *invariant closed curve bifurcates from* $B(u^*, v^*)$ *for* $h > h_2$ (*resp.*, $h < h_2$).

4 Bifurcation with 1:2 resonance

In the following, we focus on the 1:2 strong resonance bifurcation of system (4) at $B(u^*, v^*)$. Assume that

$$R_{12} = \left\{(r, k, \alpha, a, b, c, s, h) : h = h_1 = \frac{H}{(2+G)(2-s)}, s = s_1 = G + 4\right\}.$$

The two roots of (6) are $\lambda_{1,2} = -1$ when all the parameters are located in R_{12}. Then $B(u^*, v^*)$ may be a 1:2 strong resonance bifurcation point if h and s respectively vary in a small neighborhood of $h = h_1$ and $s = s_1$. We consider h and s as bifurcation parameters and assume that $(r, k, \alpha, a, b, c, s, h)$ varies in a small neighborhood of R_{12}. For convenience, we denote

$$\beta = (h, s), \qquad \beta_0 = (h_1, s_1).$$

Let $x_n = u_n - u^*$ and $y_n = v_n - v^*$. Then we transform $B(u^*, v^*)$ of system (4) into the origin and get the following form:

$$\begin{cases} x_{n+1} = (x_n + u^*)\exp(r(1 - \frac{x_n+u^*}{k}) - \frac{\alpha(y_n+v^*)}{a+b(x_n+u^*)+c(y_n+v^*)}) - u^*, \\ y_{n+1} = (y_n + v^*)\exp(s(1 - \frac{h(y_n+v^*)}{x_n+u^*})) - v^*. \end{cases} \tag{20}$$

By expanding the right-hand side of (20) into the Taylor series at the origin, we get

$$\begin{cases} x_{n+1} = \theta_1(\beta)x_n + \theta_2(\beta)y_n + N_1(x_n, y_n) + O((|x_n| + |y_n|)^4), \\ y_{n+1} = \sigma_1(\beta)x_n + \sigma_2(\beta)y_n + N_2(x_n, y_n) + +O((|x_n| + |y_n|)^4), \end{cases} \tag{21}$$

where

$$\theta_1(\beta) = c_{11}, \qquad \theta_2(\beta) = c_{12}, \qquad \sigma_1(\beta) = c_{21}, \qquad \sigma_2(\beta) = c_{22},$$

$$N_1(x_n, y_n) = \sum_{2\le i+j\le 3} \theta_{ij}(\beta)x_n^i y_n^j, \qquad N_2(x_n, y_n) = \sum_{2\le i+j\le 3} \sigma_{ij}(\beta)x_n^i y_n^j,$$

with

$$\theta_{20}(\beta) = c_{13}, \qquad \theta_{11}(\beta) = c_{14}, \qquad \theta_{02}(\beta) = c_{15},$$

$$\theta_{30}(\beta) = c_{16}, \qquad \theta_{21}(\beta) = c_{17}, \qquad \theta_{12}(\beta) = c_{18}, \qquad \theta_{03}(\beta) = c_{19},$$
$$\sigma_{20}(\beta) = c_{23}, \qquad \sigma_{11}(\beta) = c_{24}, \qquad \sigma_{02}(\beta) = c_{25},$$
$$\sigma_{30}(\beta) = c_{26}, \qquad \sigma_{21}(\beta) = c_{27}, \qquad \sigma_{12}(\beta) = c_{28}, \qquad \sigma_{03}(\beta) = c_{29}.$$

Let us define

$$A(\beta) = \begin{pmatrix} \theta_1(\beta) & \theta_2(\beta) \\ \sigma_1(\beta) & \sigma_2(\beta) \end{pmatrix}.$$

Note that we have

$$A(\beta_0) = \begin{pmatrix} s_1 - 3 & -\frac{(s_1-2)^2 h_1}{s_1} \\ \frac{s_1}{h_1} & 1 - s_1 \end{pmatrix}.$$

Moreover, there are two linearly independent eigenvectors $q_{0,1}$ of $A(\beta_0)$ and adjoint eigenvectors $p_{0,1}$ of $A^T(\beta_0)$ such that

$$A(\beta_0)q_0 = -q_0, \qquad A(\beta_0)q_1 = -q_1 + q_0,$$
$$A^T(\beta_0)p_1 = -p_1, \qquad A^T(\beta_0)p_0 = -p_0 + p_1,$$
$$\langle q_0, p_0\rangle = \langle q_1, p_1\rangle = 1, \qquad \langle q_1, p_0\rangle = \langle q_0, p_1\rangle = 0,$$

where

$$q_0 = \begin{pmatrix} \frac{h_1(s_1-2)}{s_1} \\ 1 \end{pmatrix}, \qquad q_1 = \begin{pmatrix} \frac{h_1}{s_1} \\ 0 \end{pmatrix}, \qquad p_0 = \begin{pmatrix} 0 \\ 1 \end{pmatrix}, \qquad p_1 = \begin{pmatrix} \frac{s_1}{h_1} \\ 2 - s_1 \end{pmatrix},$$

and $\langle \cdot, \cdot \rangle$ stands for the standard scalar product.

Therefore, any vector $(x_n, y_n)^T$ can be decomposed as

$$(x_n, y_n)^T = \hat{x}_n q_0 + \hat{y}_n q_1, \tag{22}$$

where the new coordinates $(\hat{x}_n, \hat{y}_n)$ are as follows:

$$\begin{cases} \hat{x}_n = \langle (x_n, y_n)^T, p_0\rangle, \\ \hat{y}_n = \langle (x_n, y_n)^T, p_1\rangle. \end{cases} \tag{23}$$

In the new coordinates $(\hat{x}_n, \hat{y}_n)$, system (21) can be written as

$$\begin{cases} \hat{x}_{n+1} = (-1 + \theta_{10}(\beta))\hat{x}_n + (1 + \theta_{01}(\beta))\hat{y}_n + \hat{N}_1(\hat{x}_n, \hat{y}_n) + O((|\hat{x}_n| + |\hat{y}_n|)^4), \\ \hat{y}_{n+1} = \sigma_{10}(\beta)\hat{x}_n + (-1 + \sigma_{01}(\beta))\hat{y}_n + \hat{N}_2(\hat{x}_n, \hat{y}_n) + +O((|\hat{x}_n| + |\hat{y}_n|)^4), \end{cases} \tag{24}$$

where

$$\theta_{10}(\beta) = \big\langle p_0, \big[A(\beta) - A(\beta_0)\big]q_0\big\rangle = 2 - s + \frac{sh_1(s_1 - 2)}{hs_1},$$
$$\theta_{01}(\beta) = \big\langle p_0, \big[A(\beta) - A(\beta_0)\big]q_1\big\rangle = -1 + \frac{sh_1}{hs_1},$$

$$
\begin{aligned}
\sigma_{10}(\beta) &= \langle p_1, [A(\beta) - A(\beta_0)]q_0 \rangle \\
&= \left[\frac{s_1}{h_1}\theta_1 + (2-s_1)\sigma_1\right]\frac{h_1(s_1-2)}{s_1} + \left[\frac{s_1}{h_1}\theta_2 + (2-s_1)\sigma_2\right], \\
\sigma_{01}(\beta) &= \langle p_1, [A(\beta) - A(\beta_0)]q_1 \rangle = 1 + \left[\frac{s_1}{h_1}\theta_1 + (2-s_1)\sigma_1\right]\frac{h_1}{s_1}, \\
\hat{N}_1(\hat{x}_n, \hat{y}_n) &= \sum_{2\le i+j\le 3} \hat{\theta}_{ij}(\beta)\hat{x}_n^i\hat{y}_n^j = N_2\left(\frac{h_1(s_1-2)}{s_1}\hat{x}_n + \frac{h_1}{s_1}\hat{y}_n, \hat{x}_n\right), \\
\hat{N}_2(\hat{x}_n, \hat{y}_n) &= \sum_{2\le i+j\le 3} \hat{\sigma}_{ij}(\beta)\hat{x}_n^i\hat{y}_n^j \\
&= \frac{s_1}{h_1}N_1\left(\frac{h_1(s_1-2)}{s_1}\hat{x}_n + \frac{h_1}{s_1}\hat{y}_n, \hat{x}_n\right) + (2-s_1)N_2\left(\frac{h_1(s_1-2)}{s_1}\hat{x}_n + \frac{h_1}{s_1}\hat{y}_n, \hat{x}_n\right).
\end{aligned}
$$

Clearly,

$$
\theta_{10}(\beta_0) = \theta_{01}(\beta_0) = \sigma_{10}(\beta_0) = \sigma_{01}(\beta_0) = 0.
$$

By introducing the nonsingular linear coordinate transformation as follows:

$$
\begin{pmatrix} \hat{x}_n \\ \hat{y}_n \end{pmatrix} = P(\beta)\begin{pmatrix} \tilde{x}_n \\ \tilde{y}_n \end{pmatrix} = \begin{pmatrix} 1+\theta_{01}(\beta) & 0 \\ -\theta_{10}(\beta) & 1 \end{pmatrix}\begin{pmatrix} \tilde{x}_n \\ \tilde{y}_n \end{pmatrix}, \tag{25}
$$

(24) can be rewritten as

$$
\begin{cases}
\tilde{x}_{n+1} = -\tilde{x}_n + \tilde{y}_n + \tilde{N}_1(\tilde{x}_n, \tilde{y}_n) + O((|\tilde{x}_n| + |\tilde{y}_n|)^4), \\
\tilde{y}_{n+1} = \tau_1(\beta)\tilde{x}_n + (-1+\tau_2(\beta))\tilde{y}_n + \tilde{N}_2(\tilde{x}_n, \tilde{y}_n) + O((|\tilde{x}_n| + |\tilde{y}_n|)^4),
\end{cases} \tag{26}
$$

where

$$
\begin{aligned}
\tau_1(\beta) &= \sigma_{01}(\beta) + \theta_{01}(\beta)\sigma_{10}(\beta) - \theta_{10}(\beta)\sigma_{01}(\beta), \\
\tau_2(\beta) &= \theta_{10}(\beta) + \sigma_{01}(\beta), \\
\tilde{N}_1(\tilde{x}_n, \tilde{y}_n) &= \sum_{2\le i+j\le 3} \tilde{\theta}_{ij}(\beta)\tilde{x}_n^i\tilde{y}_n^j = \frac{1}{1+\theta_{01}(\beta)}\hat{N}_1\big(\big(1+\theta_{01}(\beta)\big)\tilde{x}_n, -\theta_{10}(\beta)\tilde{x}_n + \tilde{y}_n\big), \\
\tilde{N}_2(\tilde{x}_n, \tilde{y}_n) &= \sum_{2\le i+j\le 3} \tilde{\sigma}_{ij}(\beta)\tilde{x}_n^i\tilde{y}_n^j \\
&= \theta_{10}(\beta)\hat{N}_1\big(\big(1+\theta_{01}(\beta)\big)\tilde{x}_n, -\theta_{10}(\beta)\tilde{x}_n + \tilde{y}_n\big) \\
&\quad + \big(1+\theta_{01}(\beta)\big)\hat{N}_2\big(\big(1+\theta_{01}(\beta)\big)\tilde{x}_n, -\theta_{10}(\beta)\tilde{x}_n + \tilde{y}_n\big).
\end{aligned}
$$

To reduce (26) to a 1:2 resonance bifurcation normal form, we introduce the following transformation:

$$
\begin{cases}
\tilde{x}_n = \xi_n + \sum_{2\le i+j\le 3} \psi_{ij}(\beta)\xi_n^i\eta_n^j, \\
\tilde{y}_n = \eta_n + \sum_{2\le i+j\le 3} \phi_{ij}(\beta)\xi_n^i\eta_n^j,
\end{cases} \tag{27}
$$

where ψ_{ij} and ϕ_{ij} will be determined later.

By using (27) and its inverse transformation, system (26) becomes of the following form:

$$\begin{cases} \xi_{n+1} = -\xi_n + \eta_n + \sum_{2\le i+j\le 3} \gamma_{ij}(\beta)\xi_n^i\eta_n^j + O((|\xi_n| + |\eta_n|)^4), \\ \eta_{n+1} = \tau_1(\beta)\xi_n + (-1 + \tau_2(\beta))\eta_n + \sum_{2\le i+j\le 3} \rho_{ij}(\beta)\xi_n^i\eta_n^j + O((|\xi_n| + |\eta_n|)^4), \end{cases} \tag{28}$$

where

$$\begin{aligned} \gamma_{20}(\beta) &= \tilde{\theta}_{20} + \phi_{20} - 2\psi_{20} - \tau_1^2\psi_{02} + \tau_1\psi_{11}, \\ \gamma_{11}(\beta) &= \tilde{\theta}_{11} + \phi_{11} - 2\tau_1(1+\tau_2)\psi_{02} + (\tau_2 - \tau_1)\psi_{11} + 2\psi_{20}, \\ \gamma_{02}(\beta) &= \tilde{\theta}_{02} + \phi_{02} - \left(1 + (1+\tau_2)^2\right)\psi_{02} + (1+\tau_2)\psi_{11} - \psi_{20}, \\ \rho_{20}(\beta) &= \tilde{\sigma}_{20} - \tau_1^2\phi_{02} + \tau_1\phi_{11} + (\tau_1 + \tau_2)\phi_{20}, \\ \rho_{11}(\beta) &= \tilde{\sigma}_{11} - 2\tau_1(1+\tau_2)\phi_{02} + (2 - \tau_1 + 2\tau_2)\phi_{11} + 2\phi_{20} + \tau_1\psi_{11}, \\ \rho_{02}(\beta) &= \tilde{\sigma}_{20} - \tau_2(1+\tau_2)\phi_{02} - (1+\tau_2)\phi_{11} - \phi_{20} + \tau_1\psi_{02}. \end{aligned}$$

To eliminate all quadratic terms in the map (28), we take

$$\gamma_{20} = \gamma_{11} = \gamma_{02} = \rho_{20} = \rho_{11} = \rho_{02} = 0,$$

then the coefficients ψ_{ij} and ϕ_{ij} for $i + j = 2$ can be computed (see the details in [28]). Similarly, the coefficients ψ_{ij} and ϕ_{ij} for $i + j = 3$ can be determined by assuming

$$\gamma_{30} = \gamma_{12} = \gamma_{21} = \gamma_{03} = \rho_{12} = \rho_{21} = \rho_{03} = 0.$$

Therefore, map (20) can be transformed into the 1:2 strong resonance bifurcation normal form as follows:

$$\begin{cases} \xi_{n+1} = -\xi_n + \eta_n + O((|\xi_n| + |\eta_n|)^4), \\ \eta_{n+1} = \tau_1(\beta)\xi_n + (-1 + \tau_2(\beta))\eta_n + C_1(\beta)\xi_n^3 + D_1(\beta)\xi_n^2\eta_n + O((|\xi_n| + |\eta_n|)^4), \end{cases} \tag{29}$$

with $C_1(\beta)$ and $D_1(\beta)$ satisfying

$$\begin{aligned} C_1(\beta_0) &= \tilde{\sigma}_{30}(\beta_0) + \tilde{\theta}_{20}(\beta_0)\tilde{\sigma}_{20}(\beta_0) + \frac{1}{2}\tilde{\sigma}_{20}^2(\beta_0) + \frac{1}{2}\tilde{\sigma}_{20}(\beta_0)\tilde{\sigma}_{11}(\beta_0), \\ D_1(\beta_0) &= \tilde{\sigma}_{21}(\beta_0) + 3\tilde{\theta}_{30}(\beta_0) + \frac{1}{2}\tilde{\theta}_{20}(\beta_0)\tilde{\sigma}_{11}(\beta_0) + \frac{5}{4}\tilde{\sigma}_{20}(\beta_0)\tilde{\sigma}_{11}(\beta_0) \\ &\quad + \tilde{\sigma}_{20}(\beta_0)\tilde{\sigma}_{02}(\beta_0) + 3\tilde{\theta}_{20}^2(\beta_0) + \frac{5}{2}\tilde{\theta}_{20}(\beta_0)\tilde{\sigma}_{20}(\beta_0) \\ &\quad + \frac{5}{2}\tilde{\theta}_{11}(\beta_0)\tilde{\sigma}_{20}(\beta_0) + \tilde{\sigma}_{20}^2(\beta_0) + \frac{1}{2}\tilde{\sigma}_{11}^2(\beta_0). \end{aligned}$$

According to the results given in [28], the parameter conditions for the 1:2 strong resonance bifurcation are presented as follows.

Theorem 4.1 *If $C_1(\beta_0) \neq 0$ and $D_1(\beta_0) + 3C_1(\beta_0) \neq 0$, then system (4) undergoes a 1:2 strong resonance bifurcation at $B(u^*, v^*)$ when parameters vary in a small neighborhood of R_{12}.*

Moreover, if $C_1(\beta_0) < 0$ (*resp.*, $C_1(\beta_0) > 0$), *then* $B(u^*, v^*)$ *is a saddle* (*resp.*, *elliptic*), *and* $D_1(\beta_0) + 3C_1(\beta_0)$ *determines the bifurcation scenario under perturbations. Furthermore, system* (4) *has the bifurcation behaviors as follows*:

(i) *There is a pitchfork bifurcation curve* $PF = \{(\tau_1, \tau_2) : \tau_1 = 0\}$, *and there exist nontrivial equilibria for* $\tau_1 < 0$;

(ii) *There is a nondegenerate Hopf bifurcation curve*

$$HP = \left\{(\tau_1, \tau_2) : \tau_1 = -\tau_2 + O\left(\left(|\tau_1| + |\tau_2|\right)^2\right), \tau_1 < 0\right\};$$

(iii) *There is a heteroclinic bifurcation curve*

$$HL = \left\{(\tau_1, \tau_2) : \tau_1 = -\frac{5}{3}\tau_2 + O\left(\left(|\tau_1| + |\tau_2|\right)^2\right), \tau_1 < 0\right\}.$$

5 Numerical simulations

Bifurcation diagrams, maximum Lyapunov exponents, and phase portraits of system (4) are presented to demonstrate the above analytic results and to explore the complex dynamical behaviors. Therefore, we consider the bifurcation parameters for the following three cases:

(i) Changing h in the interval $(12, 22)$ and specifying $r = 3$, $k = 50$, $\alpha = 0.86$, $a = 0.8$, $b = 0.1$, $c = 0.05$, $s = 0.4$;

(ii) Changing h in the interval $(3, 11)$ and specifying $r = 3$, $k = 50$, $\alpha = 0.86$, $a = 0.8$, $b = 0.1$, $c = 0.05$, $s = 1.2$;

(iii) Changing h in the interval $[1.22, 1.24]$ and s in the interval $[0.5, 0.7]$, and specifying $r = 10$, $k = 50$, $\alpha = 0.86$, $a = 0.8$, $b = 0.1$, $c = 0.05$.

For case (i). When $h = h_1 = 14.44845$, the unique positive fixed point is $B(u^*, v^*) = (41.905164, 2.900322)$ and the eigenvalues of (5) are $\lambda_1 = -1$ and $\lambda_2 = 0.482006$. In addition, $s \neq G + 4 = 1.882005$ and $\mu_1 = 0.04465407588 \neq 0$, $\mu_2 = 0.057614 > 0$. Then we know from Theorem 3.1 that a stable period-2 orbit emerges from the unique positive fixed point $B(u^*, v^*)$. The bifurcation diagrams for (h, u) and (h, v) are displayed in Fig. 1(a) and (b), respectively. The maximum Lyapunov exponents corresponding to Fig. 1(a) and (b) are shown in Fig. 1(c). From Fig. 1(a) and (b), the unique positive point $B(u^*, v^*)$ is stable for $12 < h < h_1$ and loses its stability at the flip bifurcation parameter value $h = h_1$. Meanwhile, we can observe complex dynamical behaviors such as a cascade of period-doubling, period-10 orbits, quasi-periodic orbits, periodic windows, and chaos (see Figs. 1 and 2). Figure 2 shows some phase portraits associated with Fig. 1(a) and (b). If $h = 21$, a chaotic set is observed and its maximum Lyapunov exponent verifies the existence of the chaotic set. According to Fig. 1, when the number of prey required to support a predator is less than 18.7988, the dynamical behavior of system (4) is stable and chaos does not occur. Moreover, the dynamical behavior of system (4) stabilizes when the number of prey required to support a predator becomes small.

For case (ii). When $h = h_2 = 8.9081$, the unique positive fixed point is $B(u^*, v^*) = (37.33459221, 4.191083644)$ and the eigenvalues of system (5) are $\lambda_1 = -0.4209507970 + i0.9070834805$ and $\lambda_2 = \bar{\lambda_1}$. Furthermore, we can get $|\lambda_{1,2}| = 1$. Additionally, $G = -1.641901594 \neq s - 1, s - 2$ and $l = -0.03712915975 < 0$. Then we know from Theorem 3.2 that the Hopf bifurcation occurs and an attracting invariant cycle emerges from the unique

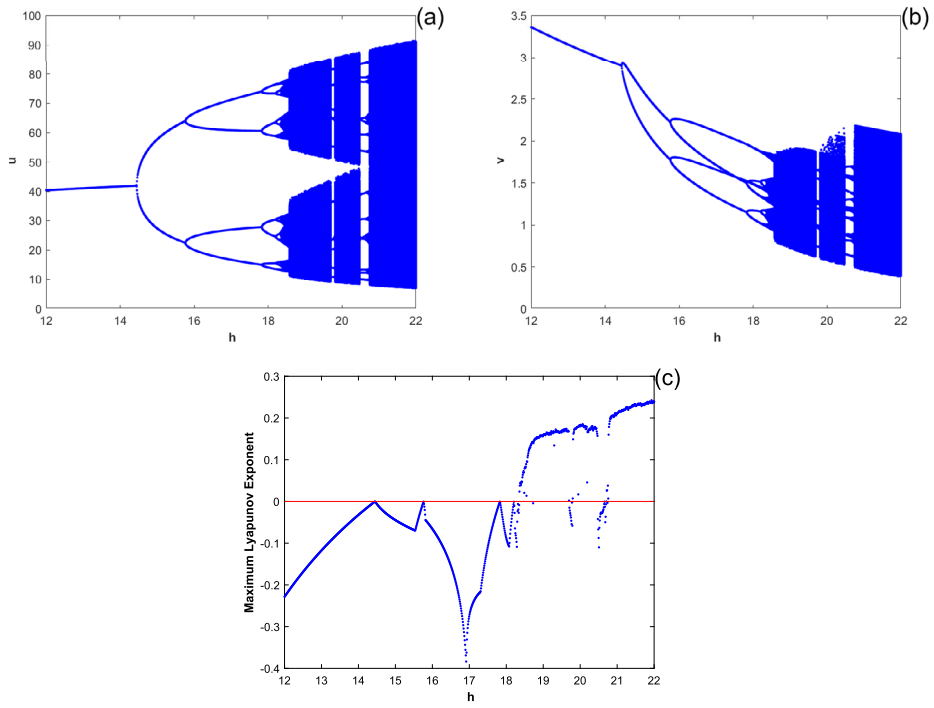

Figure 1 (a) Flip bifurcation diagram of system (4) in the (h, u) plane with the initial value $(u_0, v_0) = (8, 2)$. (b) Flip bifurcation diagram of system (4) in the (h, v) plane. (c) Maximum Lyapunov exponents corresponding to (a) and (b)

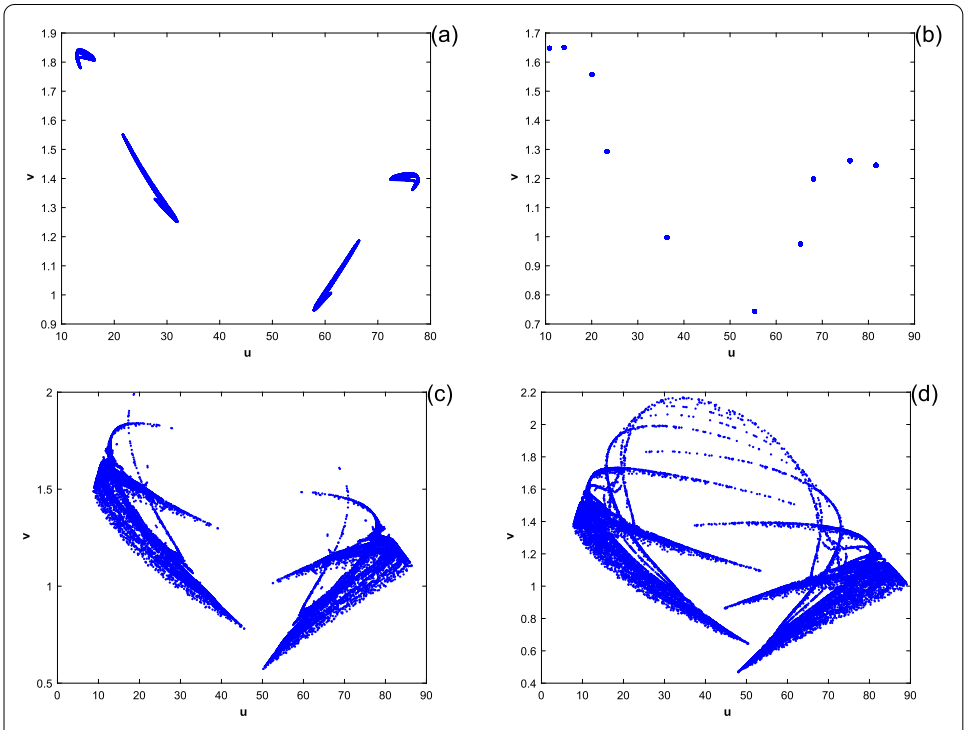

Figure 2 Phase portraits corresponding to Fig. 2(a) and (b). (a)Quasi-periodic orbits for $h = 18.5$. (b) Period-10 orbits for $h = 19.7$. (c) Quasi-periodic orbits $h = 20$. (d) A chaotic attractor for $h = 21$

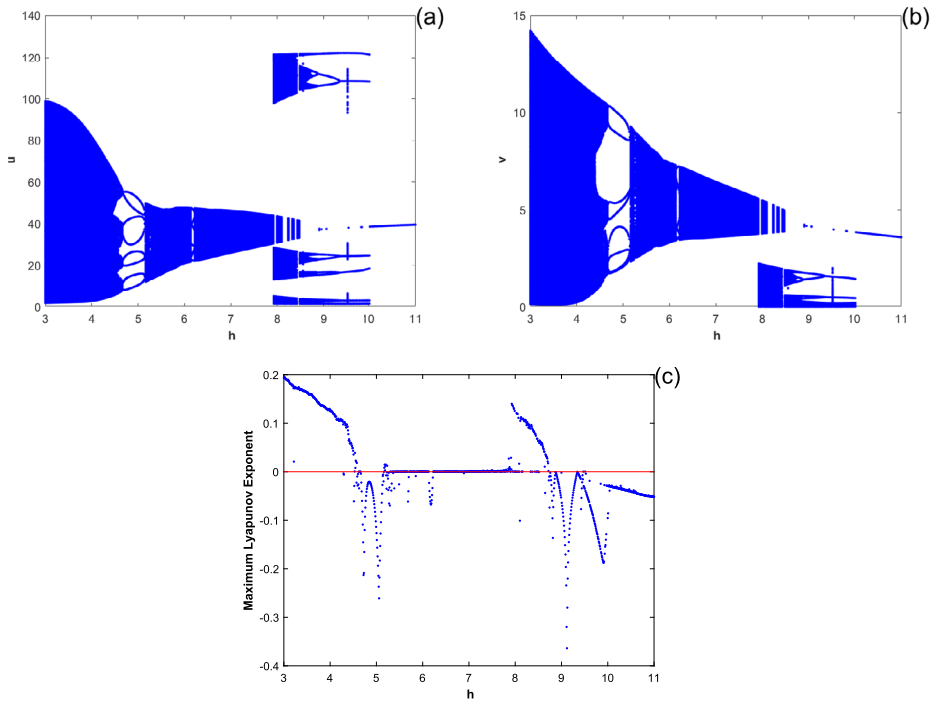

Figure 3 (a) Hopf bifurcation diagram of system (4) in the (h, u) plane with the initial value $(u_0, v_0) = (8, 2)$. (b) Hopf bifurcation diagram of system (4) in the (h, v) plane. (c) Maximum Lyapunov exponents corresponding to (a) and (b)

fixed point $B(u^*, v^*)$. The bifurcation diagrams for (h, u) and (h, v) are displayed in Fig. 3(a) and (b), respectively. The maximum Lyapunov exponents corresponding to Fig. 3(a) and (b) are shown in Fig. 3(c). Figure 4 displays the phase portraits of system (4) corresponding to Fig. 3(a) and (b). It can be observed from Fig. 4 that there are period-6, period-12, an invariant closed curve, and an attracting chaotic set. Meanwhile, when a chaotic attractor happens for $h = 4$, the maximum Lyapunov exponent from Fig. 3(c) confirms its existence. According to Fig. 3, when the number of prey required to support a predator becomes large, the dynamical behavior of system (4) will tend to be stable.

For case (iii). When $h = h_1 = 1.237988529$ and $s = s_1 = 0.6123350405$, the unique positive fixed point is $B(u^*, v^*) = (29.28847604, 23.65811586)$ and the eigenvalues of system (5) at $B(u^*, v^*)$ are $\lambda_1 = \lambda_2 = -1$. Furthermore, we can obtain $C_1(\beta_0) = 0.2700889125$ and $D_1(\beta_0) + 3C_1(\beta_0) = 1.412346912$. According to Theorem 4.1, system (4) can undergo a 1:2 resonance at the unique positive fixed point $B(u^*, v^*)$ when the parameters h and s vary in the neighborhood of (h_1, s_1). The 2-dimensional bifurcation diagram for (s, u) is presented in Fig. 5(a) when $h = h_1$ and s varies in a neighborhood of s_1. Figure 5(b) shows the 3-dimensional bifurcation diagram for (h, s, u) when (h, s) varies in a neighborhood of (h_1, s_1). The phase portraits of system (4) near $B(u^*, v^*)$ for different parameters h and s are shown in Fig. 6(a)–(d). When h and s vary in the neighborhood of (h_1, s_1), system (4) presents complex dynamical behaviors such as period-7 orbits, invariant curves, and an attractor.

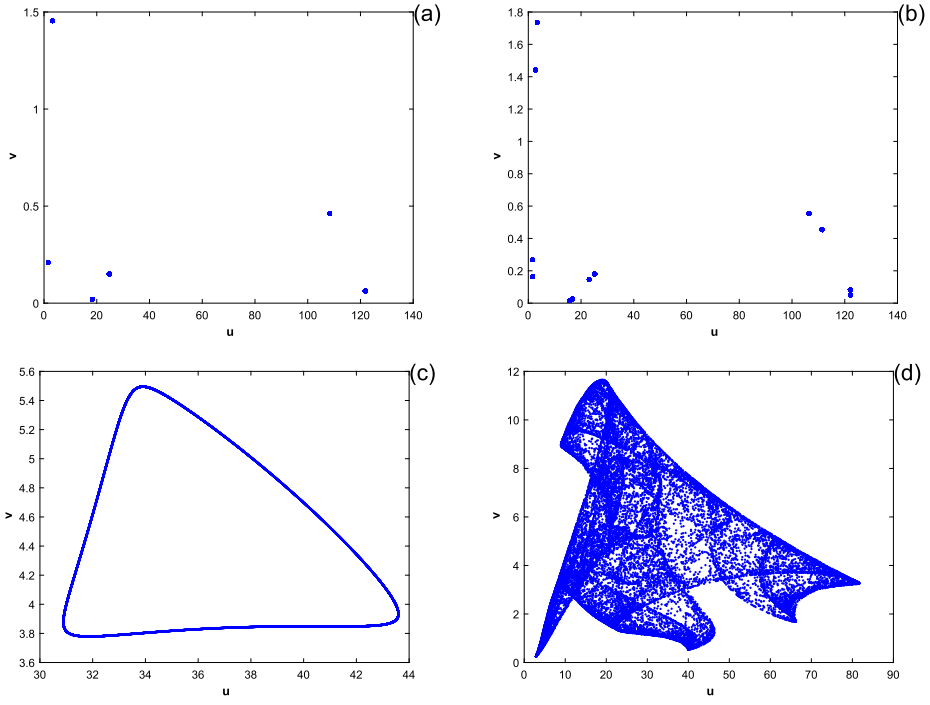

Figure 4 Phase portraits corresponding to Fig. 3 (a) and (b). (a) Period-6 orbits for $h = 10$. (b) Period-12 orbits for $h = 9$. (c) An attracting invariant cycle for $h = 8$. (d) A chaotic attractor for $h = 4$

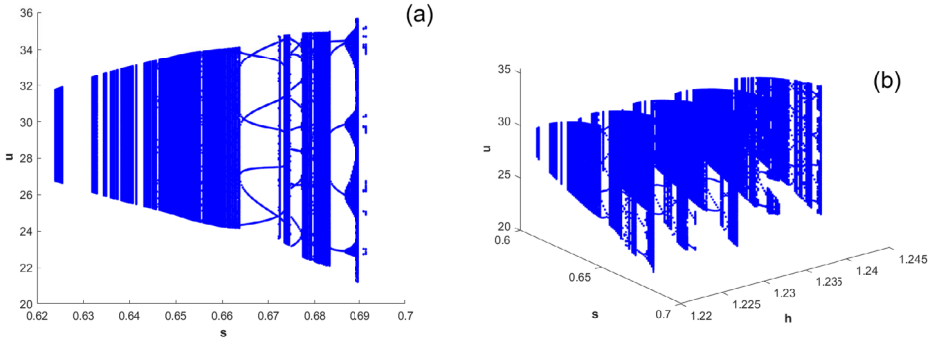

Figure 5 Bifurcation diagram of system (4) near the fixed point $B(29.2885, 23.6581)$. (a) On the (s,u)-plane, where $h = 1.23$ and $0.5 \le s \le 0.7$. (b) In the (h,s,u) space, where $1.22 \le h \le 1.24$ and $0.5 \le s \le 0.7$

6 Chaos control

In this section, the state feedback control method will be used to stabilize the chaotic set of system (4). Then we consider the following controlled map:

$$\begin{cases} u_{n+1} = u_n \exp(r(1 - \frac{u_n}{k}) - \frac{\alpha v_n}{a+bu_n+cv_n}) + w(u_n, y_n), \\ v_{n+1} = v_n \exp(s(1 - \frac{hv_n}{u_n})), \end{cases} \tag{30}$$

where $w(u_n, u_n) = -\mu_1(u_n - u^*) - \mu_2(v_n - v^*)$ is the feedback controlling force and μ_1, μ_2 represent the feedback gains.

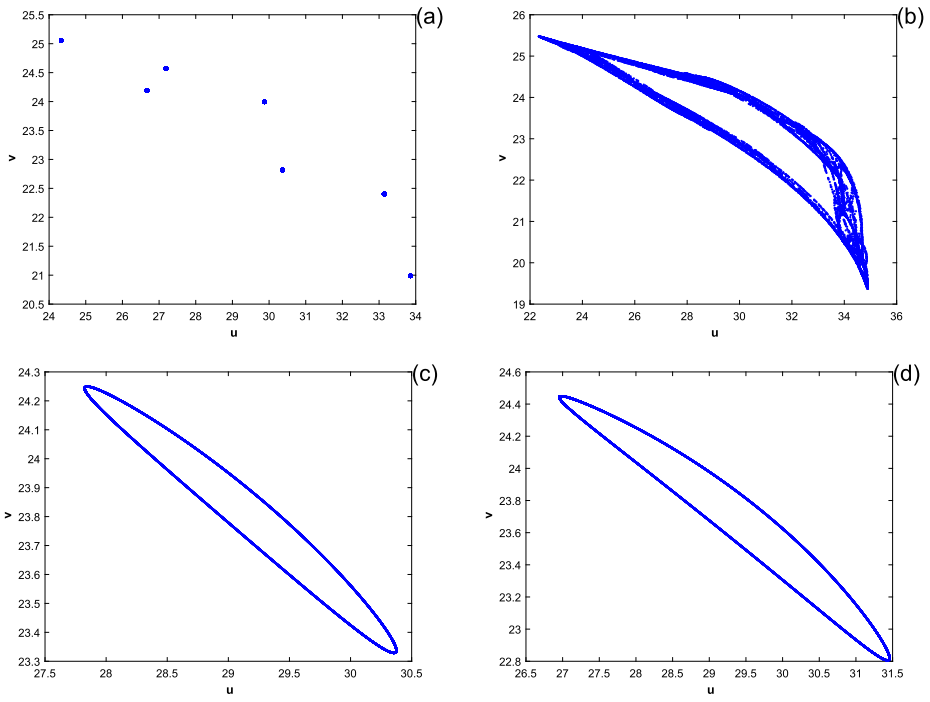

Figure 6 Phase portraits of system (4) for various values of h and s. (a) $h = 1.23$, $s = 0.664$. (b) $h = 1.23$, $s = 0.68$. (c) $h = 1.22$, $s = 0.61$. (d) $h = 1.226$, $s = 0.62$

The Jacobian matrix of map (30) at $B(u^*, v^*)$ is

$$J(u^*, v^*) = \begin{pmatrix} c_{11} - \mu_1 & c_{12} - \mu_2 \\ c_{21} & c_{22} \end{pmatrix}.$$

The characteristic equation of $J(u^*, v^*)$ is

$$\lambda^2 - (c_{11} + c_{22} - \mu_1)\lambda + c_{22}(c_{11} - \mu_1) - c_{21}(c_{12} - \mu_2). \tag{31}$$

If λ_1 and λ_2 are the eigenvalues of (31), then we obtain

$$\lambda_1 + \lambda_2 = c_{11} + c_{22} - \mu_1, \lambda_1\lambda_2 = c_{22}(c_{11} - \mu_1) - c_{21}(c_{12} - \mu_2). \tag{32}$$

By solving the equations $\lambda_1 = \pm 1$, the lines of marginal stability can be gotten. Moreover, these restricted conditions assure $|\lambda_{1,2}| < 1$.

According to (32), $\lambda_1\lambda_2 = 1$ implies that

$$L_1 : \mu_1 c_{22} - \mu_2 c_{21} = c_{11}c_{22} - c_{12}c_{21} - 1. \tag{33}$$

According to (32), $\lambda_1 = 1$ deduces that

$$L_2 : \mu_1(1 - c_{22}) + \mu_2 c_{21} = c_{11} + c_{22} - 1 - c_{11}c_{22} + c_{12}c_{21}. \tag{34}$$

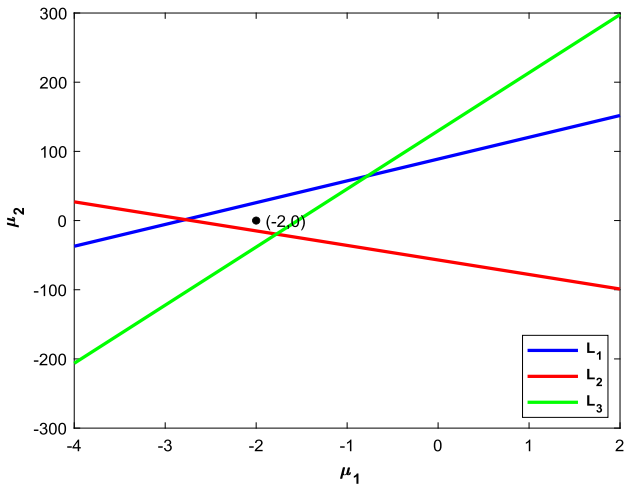

Figure 7 The bounded region for the eigenvalues of controlled system (30) in the (μ_1, μ_2) plane. Clearly, the point $(-2, 0)$ is in the stability region of (30)

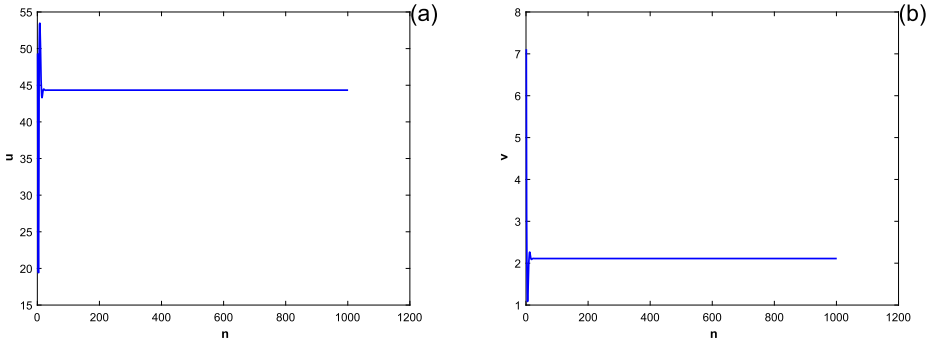

Figure 8 (a) The time responses for the prey of controlled system (30). (b) The time responses for the predator of controlled system (30)

Furthermore, assume that $\lambda_1 = -1$ deduces that

$$L_3 : \mu_1(1 + c_{22}) - \mu_2 c_{21} = c_{11} + c_{22} - 1 + c_{11}c_{22} - c_{12}c_{21}. \tag{35}$$

Therefore, the stable eigenvalues of map (30) at $B(u^*, v^*)$ will lie within the triangular region bounded by L_1, L_2, and L_3 (see Fig. 7).

From Fig. 1 and Fig. 2(d) it can be seen that system (4) exhibits chaotic behavior when $h = 21$, $r = 3$, $k = 50$, $\alpha = 0.86$, $a = 0.8$, $b = 0.1$, $c = 0.05$, $s = 0.4$. The stable eigenvalues lie within a triangular region, as depicted in Fig. 7. Select the feedback gains for $\mu_1 = -2$ and $\mu_2 = 0$. This point $(\mu_1, \mu_2) = (-2, 0)$ lies well inside the triangular region, as depicted in Fig. 7. From Fig. 8 it is shown that the chaotic trajectory stabilizes at the unique positive fixed point $B(u^*, v^*) = (44.3323, 2.1111)$.

7 Conclusion

In this paper, we have considered the complex dynamical behaviors of a discrete Holling–Tanner model with Beddington–DeAngelis functional response. The permanence and lo-

cal stability of fixed points for system (4) are derived. By using the center manifold theorem and bifurcation theory, the flip and Hopf bifurcations can occur around the unique positive fixed point if we choose suitable parameters. Furthermore, we explore the 1:2 resonance bifurcation of system (4). Numerical simulations have shown that system (4) exhibits very rich complex dynamical behaviors. The state feedback control method is used to stabilize the chaotic set of system (4). According to Fig. 1 and Fig. 3, when the intrinsic growth rate of a predator is small ($s = 0.4$), the number of prey required to support a predator becoming small will stabilize the dynamical behavior of system (4). Conversely, when the intrinsic growth rate of a predator is large ($s = 1.2$), the number of prey required to support a predator becoming large will stabilize the dynamical behavior of system (4). Compared with the continuous-time system (1) in [9], system (4) exhibits more complex dynamical behaviors such as period-6, 7, 10, 12 orbits, an attracting invariant cycle, a cascade of period-doubling, quasi-periodic orbits, and the chaotic sets. These complex dynamical behaviors imply that the coexistence of predator and prey may produce very complex stable patterns.

Acknowledgements
The authors gratefully acknowledge the referees for their useful comments on the paper.

Funding
This work was supported by Sichuan Minzu College (no. XYZB2106ZB).

Availability of data and materials
Not applicable.

Declarations

Ethics approval and consent to participate
Not applicable.

Consent for publication
Not applicable.

Competing interests
The authors declare no competing interests.

Author contributions
JZ is responsible for the model formulation and study planning. JZ and RY have done the calculation, the proof, and the simulation. Both authors have read and approved the final manuscript.

Received: 17 April 2023 Accepted: 10 October 2023 Published online: 23 October 2023

References

1. Berryman, A.A.: The origins and evolution of predator-prey theory. Ecology **73**, 1530–1535 (1992)
2. Li, W.L., Huang, J.: Globally exponentially stable periodic solution in a general delayed predator-prey model under discontinuous prey control strategy. Discrete Contin. Dyn. Syst., Ser. B **25**, 2639–2664 (2020)
3. Li, W., Ji, J., Huang, L.: Global dynamic behavior of a predator-prey model under ratio-dependent state impulsive control. Appl. Math. Model. **77**, 1842–1859 (2020)
4. Li, W., Zhang, Y., Huang, L.: Dynamics analysis of a predator–prey model with nonmonotonic functional response and impulsive control. Math. Comput. Simul. **204**, 529–555 (2023)
5. Gupta, R.: Dynamics of a Holling-Tanner model. Am. J. Eng. Res. **4**, 132–140 (2017)
6. Shi, H., Li, W., Lin, G.: Positive steady states of a diffusive predator–prey system with modified Holling–Tanner functional response. Nonlinear Anal., Real World Appl. **11**, 3711–3721 (2010)
7. Yang, W.: Global asymptotical stability and persistent property for a diffusive predator–prey system with modified Leslie–Gower functional response. Nonlinear Anal., Real World Appl. **14**, 1323–1330 (2013)
8. Zhao, J., Yan, Y.: Stability and bifurcation analysis of a discrete predator–prey system with modified Holling–Tanner functional response. Adv. Differ. Equ. **2018**, 402 (2018)
9. Li, Y., Zhang, L., Li, D., Shi, H.: Spatiotemporal dynamics of a diffusive Leslie-type predator–prey model with Beddington–DeAngelis functional response. J. Biol. Syst. **28**, 785–809 (2020)
10. Roy, B., Roy, S.K., Gurung, D.B.: Holling–Tanner model with Beddington–DeAngelis functional response and time delay introducing harvesting. Math. Comput. Simul. **142**, 1–14 (2017)

11. Din, Q.: Complexity and chaos control in a discrete-time prey-predator model. Commun. Nonlinear Sci. Numer. Simul. **49**, 113–134 (2017)
12. Cao, H., Zhou, Y., Ma, Z.: Bifurcation analysis of a discrete SIS model with bilinear incidence depending on new infection. Math. Biosci. Eng. **10**, 1399–1417 (2013)
13. Zhang, L., Zhang, C., He, Z.: Codimension-one and codimension-two bifurcations of a discrete predator–prey system with strong Allee effect. Math. Comput. Simul. **162**, 155–178 (2019)
14. Ren, J., Yu, L., Siegmund, S.: Bifurcations and chaos in a discrete predator–prey model with Crowley–Martin functional response. Nonlinear Dyn. **90**, 19–41 (2017)
15. Choo, S.: Global stability in n-dimensional discrete Lotka-Volterra predator-prey models. Adv. Differ. Equ. **2014**, 11 (2014)
16. Jana, D.: Chaotic dynamics of a discrete predator–prey system with prey refuge. Appl. Math. Comput. **224**, 848–865 (2013)
17. Huang, J., Liu, S., Ruan, S., Xiao, D.: Bifurcations in a discrete predator–prey model with nonmonotonic functional response. J. Math. Anal. Appl. **464**, 201–230 (2018)
18. Cui, Q., Zhang, Q., Qiu, Z., Hu, Z.: Complex dynamics of a discrete-time predator-prey system with Holling IV functional response. Chaos Solitons Fractals **87**, 158–171 (2016)
19. Asheghi, R.: Bifurcations and dynamics of a discrete predator–prey system. J. Biol. Dyn. **8**, 161–186 (2014)
20. Celik, C., Duman, O.: Allee effect in a discrete-time predator–prey system. Chaos Solitons Fractals **40**, 1956–1962 (2009)
21. Wang, C., Li, X.: Further investigations into the stability and bifurcation of a discrete predator–prey model. J. Math. Anal. Appl. **422**, 920–939 (2015)
22. Zhuo, X., Zhang, F.: Stability for a new discrete ratio-dependent predator–prey system. Qual. Theory Dyn. Syst. **17**, 189–202 (2018)
23. He, Z., Lai, X.: Bifurcation and chaotic behavior of a discrete-time predator–prey system. Nonlinear Anal., Real World Appl. **12**, 403–417 (2011)
24. Balreira, E.C., Elaydi, S., Luis, R.: Local stability implies global stability for the planar Ricker competition model. Discrete Contin. Dyn. Syst., Ser. B **19**, 323–351 (2014)
25. Elaydi, S., Luis, R.: Open problems in some competition models. J. Differ. Equ. Appl. **17**, 1873–1877 (2011)
26. Smith, H.L.: Planar competitive and cooperative difference equations. J. Differ. Equ. Appl. **3**, 335–357 (1998)
27. Chen, F.: Permanence for the discrete mutualism model with time delays. Math. Comput. Model. **47**, 431–435 (2008)
28. Kuznetsov, Y.: Elements of Applied Bifurcation Theory. Springer, Berlin (1998)

Publisher's Note